

## Final-state effects in the x-ray photoelectron spectra of cubic sodium-tungsten bronzes

J.-N. Chazalviel,\* M. Campagna, and G. K. Wertheim  
Bell Laboratories, Murray Hill, New Jersey 07974

H. R. Shanks

Ames Laboratory, Iowa State University, Ames, Iowa 50100

(Received 2 March 1977)

Core-electron, valence-, and conduction-band spectra of the cubic sodium-tungsten bronzes  $\text{Na}_x\text{WO}_3$  have been obtained by x-ray photoelectron spectroscopy. The samples were vacuum-cleaved single crystals spanning the entire cubic composition range. The band spectra are consistent with the theoretical band structure, and the filling of the conduction band with increasing  $x$  is explicitly demonstrated. Sodium and oxygen core-electron spectra have binding energies fixed relative to the bottom of the conduction band and exhibit the plasmon satellites expected on the basis of optical and energy-loss measurements. The unique satellite structure of the tungsten  $4f$  electrons is discussed in terms of an excitation of the conduction-band electrons during the photoemission process.

### I. INTRODUCTION

The sodium-tungsten bronzes,  $\text{Na}_x\text{WO}_3$ , are an attractive physical system for a variety of experiments because the sodium concentration spans the range  $0 < x < 1$ , providing a system that can be varied from insulating to metallic.<sup>1</sup> Above a critical concentration  $x$  of  $\sim 0.3$  these materials are metallic and the concentration of conduction electrons is equal to  $x$ . The effect of disorder in the arrangement of the sodium ions is small, as evidenced by the rather high electron mobility<sup>2</sup> and the observation of Fermi-surface effects.<sup>3</sup> The present study is limited to the cubic phase of these materials, which is stable in the range  $0.49 < x < 1$ .<sup>4</sup> As reported in a preliminary letter<sup>5</sup> the x-ray photoelectron spectra (XPS) of the core levels in these

compounds exhibit interesting satellite structures, the most puzzling behavior being that of the W  $4f$  levels. In this paper, we report a more complete experimental study of these spectra extending over the whole cubic-concentration range. The various spectra have been analyzed numerically using least-squares procedures, and the positions and relative intensities of the various satellites have been deduced. The results are discussed in the context of our current theoretical understanding.

In Sec. II, we recall the band structure of the materials. In Sec. III, we present the experimental data and the results of the analyses, with special emphasis on the W  $4f$  spectrum. In Sec. IV, two theoretical models are successively invoked to account for the structure of the W  $4f$  spectrum: the Friedel exciton and plasmon excitation. Neither is found to give satisfactory agreement, and new directions are subsequently suggested.

### II. BAND STRUCTURE OF THE TUNGSTEN BRONZES

The band structure of cubic sodium-tungsten bronzes is similar to those of  $\text{ReO}_3$  and the transition-metal perovskites, e.g.,  $\text{SrTiO}_3$ , which are now rather well established.<sup>6</sup> As shown by Wolfgram,<sup>7</sup> these band structures can be readily understood in terms of tight-binding wave functions formed by combinations of the oxygen  $2p$  and metal  $d$  (here W  $5d$ ) orbitals. If the oxygen atoms in the unit cell are labeled 1 to 3 (see Fig. 1), the basis atomic functions are  $d_i$  ( $i=1$  to 5) and  $p_{j\alpha}$  ( $j=1$  to 3,  $\alpha=x, y, z$ ). The corresponding  $14 \times 14$  Hamiltonian matrix is unexpectedly simple, because the metal  $e_g$   $5d$  states ( $i=4, 5$ ) admix only with one of the three  $p$  states of each oxygen atom (namely,  $p_{1x}, p_{2y}, p_{3z}$ ) giving rise to two pairs of  $\sigma$  bands (two bonding and two antibonding) and an oxygen flat

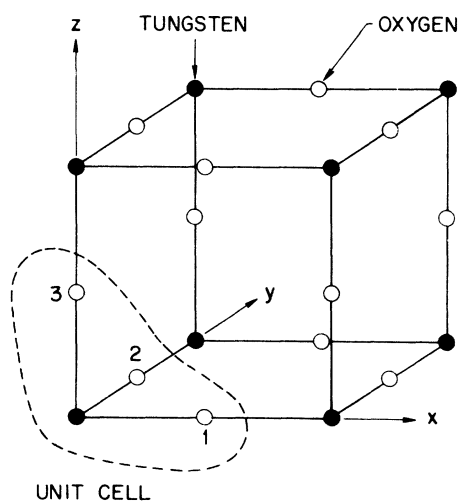


FIG. 1. Crystal structure of  $\text{Na}_x\text{WO}_3$ . Enclosed in a dashed line are the atoms forming a unit cell.

band.<sup>7</sup> On the other hand, each of the three  $t_{2g}$   $5d$  states admix only with two oxygen  $p$  states (i.e.,  $xy$  admixes with  $p_{1y}$  and  $p_{2x}$ , etc.) giving rise to three oxygen flat bands and three pairs of  $\pi$  bands. The density of states is schematized in Fig. 2. For the hypothetical cubic  $WO_3$ , the 6  $d$ -electrons from tungsten and the  $3 \times 4$  electrons from the three oxygens fill these bands up to the energy gap which lies between the O  $2p$  and W  $5d$  atomic levels. For  $Na_xWO_3$ , the fractional extra electron from the Na appears in the  $\pi$ -antibonding conduction band.

In the simplified model, where only the  $\sigma$  and  $\pi$  transfer integrals ( $S$  and  $P$ , respectively) are taken into account, that is neglecting the direct oxygen-oxygen bonding, the equation of the  $\pi$  anti-bonding band is<sup>7</sup>

$$E_{\alpha\beta}^+ = \{D^2 + 4P^2[\sin^2(\frac{1}{2}k_{\alpha}a) + \sin^2(\frac{1}{2}k_{\beta}a)]\}^{1/2}, \quad (1)$$

where the origin of the energies has been taken at  $\frac{1}{2}[E(t_{2g}) + E(p_{\perp})]$  and with  $D = \frac{1}{2}[E(t_{2g}) - E(p_{\perp})]$ . (Here, the O  $2p$  levels are split into  $p_{\perp}$  and  $p_{\parallel}$  because the oxygen environment has only axial symmetry.) The corresponding density of states is

$$\rho(E) = \frac{1}{\pi^2} \frac{E}{P^2} K\left(\frac{(E^2 - D^2)^{1/2}(8P^2 + D^2 - E^2)^{1/2}}{4P^2}\right), \quad (2)$$

where  $K(k)$  is the elliptic integral

$$\int_0^{\pi/2} \frac{dt}{(1 - k^2 \sin^2 t)^{1/2}}.$$

The wave functions are hybridized; the W  $5d$  weighting factor turns out to be simply  $(E + D)/2E$ , which is 1 at the bottom of the conduction band, and decreases slowly toward  $\frac{1}{2}$  at higher energies. This permits a calculation of the XPS yield of the conduction band

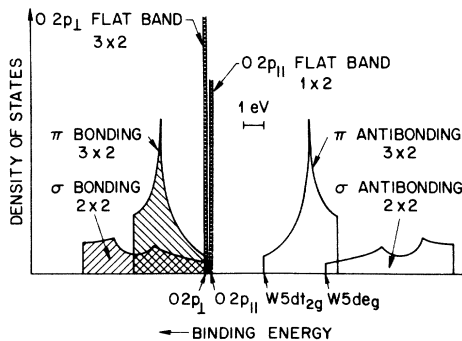


FIG. 2. Schematic density of states from the band structure of Ref. 7, with plausible parameters for  $Na_xWO_3$ . The numbers refer to the number of states, including spin degeneracy. The hatched areas show the occupied states for the hypothetical cubic  $WO_3$ . Taking into account the oxygen-oxygen transfer integrals in the Hamiltonian matrix would result in a finite width ( $\sim 1$  eV) for the oxygen flat bands.

$$f(E) \propto \left( \sigma_{W 5d} \frac{E+D}{2E} + \sigma_{O 2p} \frac{E-D}{2E} \right) \rho(E), \quad (3)$$

where  $\sigma_{W 5d}$  and  $\sigma_{O 2p}$  are the respective cross sections of the W  $5d$  and O  $2p$  atomic states.<sup>8</sup> The band is fully determined by the two parameters  $D$  and  $P$ . These are estimated to be 0.0443 and 0.1200 Ry, respectively, for  $ReO_3$ .<sup>6</sup> Comparable accurate values are not available for the bronzes. In the following, the same value of  $P$  as for  $ReO_3$  has been assumed to be reasonable and a more appropriate value for  $D$  has been deduced from the energy gap observed in the XPS:  $D$  should be about half of this gap, which gives  $D \approx 0.1$  Ry.

### III. EXPERIMENTAL: METHOD, RESULTS, AND FITTING PROCEDURES

XPS were obtained in a HP 5950A spectrometer with 0.6-eV resolution full width at half-maximum. Clean surfaces were prepared by cleaving in a vacuum better than  $10^{-8}$  Torr; the sample was then inserted into the main chamber of the spectrometer where the vacuum was in the  $10^{-9}$  range. In some cases, several samples with nominally the same  $x$  value were investigated in order to check the reproducibility of the spectra. No appreciable change was observed during the several hours extent of the experiments. The effect of air exposure on some of the samples reported here has been described elsewhere.<sup>9</sup>

All the levels accessible with the Al  $K\alpha$  x-ray energy were investigated, but we will present only the conduction and band spectra and the Na  $1s$ , O  $1s$ , and W  $4f$  core levels, which contain all the information to be discussed.

#### A. Conduction and valence bands

The band spectra for two different samples are shown superimposed in Fig. 3. The valence bands are seen to fall in almost perfect coincidence. The conduction bands coincide near the bottom, but are distinctly different near the Fermi energy. This gives evidence for the filling of the conduction band as  $x$  increases. This constitutes a further support for the homogeneous nature of the bronzes,<sup>3, 10, 11</sup> and contradicts a model recently invoked to explain their transport properties.<sup>12</sup> This change of the conduction-band spectrum with  $x$  was used in an independent determination for  $x$  for our samples (see Appendix A).

The Fermi level was accurately determined in order to obtain a good energy reference for the core levels. This was done by fitting the conduction-band spectrum with a calculated spectrum, obtained by convoluting the theoretical XPS yield [Eq. (3)] with the experimental resolution function.

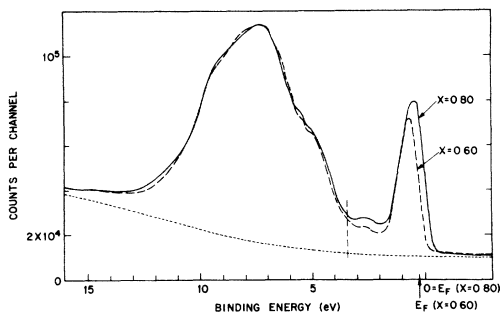


FIG. 3. Band spectra of two samples with  $x=0.60$  and  $x=0.80$ . The valence bands have been superimposed and the Fermi levels are subsequently shifted relative to each other by an amount  $\approx 0.25$  eV. The dotted line is a fitted background. The vertical dashed line is the limit of integration for measuring the relative area of the conduction band (see Appendix A). The bump in the energy gap is the  $\omega_1$  plasmon satellite of the conduction band (see Sec. III B).

The Fermi energy (relative to the bottom of the conduction band) was used as an adjustable parameter, and as expected was found to increase with  $x$ . The Fermi level was determined to an accuracy better than  $\pm 0.04$  eV.

#### B. Na 1s and O 1s core lines: the $\omega_1$ plasmon

The Na 1s and O 1s XPS can be understood as the superposition of a main line and a smaller broad satellite about 2 eV toward higher binding energy.<sup>5</sup> Unfortunately, the O 1s spectrum is further obscured by an extraneous line, which is part of the Na KLL Auger spectrum<sup>13</sup> (see Fig. 4) making a quantitative analysis difficult. The 2-eV satellite clearly originates from plasmon excitation (intrinsic and/or extrinsic). This plasmon mode of a rather low energy  $\hbar\omega_1 \sim 2$  eV, has already been observed by optical measurements<sup>14</sup> and more re-

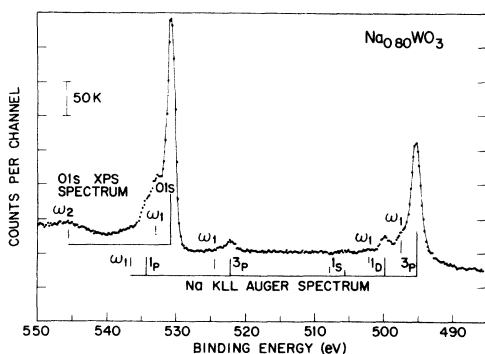


FIG. 4. O 1s XPS and Na KLL Auger spectra. Note the presence of the  $\omega_1$  plasmon satellite for every line. The appearance of these two spectra in the same energy range makes the analysis of the O 1s structure difficult.

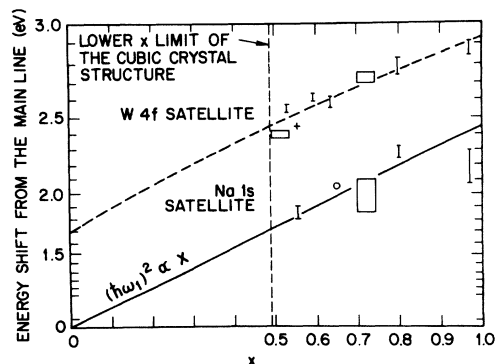


FIG. 5. Energy shifts  $\Delta E$  of the Na 1s satellite and W 4f satellite, relative to the fundamental line, as a function of  $x$ . The vertical scale is quadratic and permits to check the behavior  $\Delta E \propto x^{1/2}$  for the Na 1s satellite, as expected for plasmons ( $\Delta E = \hbar\omega_1$ ). The point shown as a circle is from the optical data of Ref. 14. The W 4f satellite clearly has a distinct  $\Delta E$ , which might be understood as due to a "bound plasmon" or a "Friedel exciton" [see the dashed line, of equation  $\Delta E = -E_B + E_F(x)$ , where binding energy of the exciton is  $E_B = -1.7$  eV].

cently by electron-energy-loss spectroscopy.<sup>15</sup> It probably plays a major role in the coloration of the bronzes. It can be understood as a collective excitation of the conduction electrons, whose small concentration ( $x < 1$ ) can explain the small energy of  $\hbar\omega_1$ . The plasmon mode corresponding to the collective excitation of both the conduction and valence electrons is observed at a higher energy  $\hbar\omega_2 \approx 15$  eV. By fitting the Na 1s XPS data, we have been able to extract the plasmon energy  $\hbar\omega_1$  for several values of  $x$ . The results are plotted in Fig. 5. The law  $\omega_1^2 \propto x$ , which one would expect—at least in a parabolic model of the band—seems to be obeyed within the experimental uncertainties.

The  $\omega_1$  plasmon manifests itself on most of the XPS lines in the spectrum, and also on the Na KLL Auger lines, as can be seen from Fig. 4. It is also present in the spectrum of the conduction band where it appears as a bump in the region of the gap (Fig. 3). The dependence of this feature upon  $x$  supports its assignment to the  $\omega_1$  plasmon, as any hypothetical level in the gap would give an  $x$ -independent contribution.

#### C. Special case of the W 4f spectrum

The W 4f spectrum can also be decomposed into two components—fundamental and satellite—but the satellite intensity appears to be unusually large. This spectrum is additionally complicated because each component is itself split into two multiplet lines,  ${}^2F_{7/2}$  and  ${}^2F_{5/2}$ , separated by the spin-orbit splitting of 2.20 eV. This results in the compli-

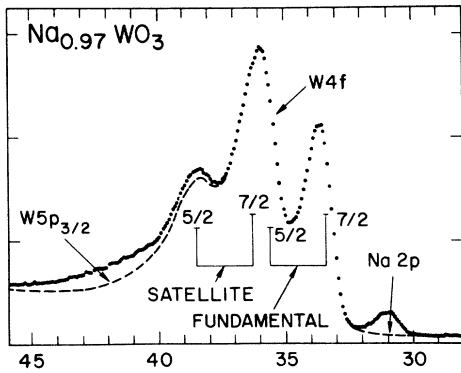


FIG. 6. W 4f XPS for a typical sample with  $x=0.97$ . The points are the original data; the dashed line is after subtraction of the estimated contributions of the W  $5p_{3/2}$  and Na  $2p$  levels (see text and Appendix B).

cated shape displayed in Fig. 6, which requires care in data analysis. Two approaches were used: (i) a spin-orbit stripping technique which separates the  ${}^2F_{7/2}$  part; and (ii) least-squares fitting of the original data with a set of four lines.

#### 1. Analysis using spin-orbit stripping

As a preliminary method of analysis, the  ${}^2F_{5/2}$  part was subtracted from the spectrum by using a standard stripping technique. This method is especially attractive because it is simple and fast. The only assumptions are that the  ${}^5_2$  and  ${}^7_2$  parts have the same shape (whatever it might be) with an intensity ratio of 3 to 4, and a separation equal to the known spin-orbit splitting of 2.20 eV. A small complication, however, was caused by the appearance of the W  $5p_{3/2}$  line in the immediate vicinity of the W 4f peaks.<sup>16</sup> A procedure developed to subtract this small extraneous contribution from the original data is described in Appendix B. Figure 7 shows some representative results of the spin-orbit-stripping technique, with and without W  $5p_{3/2}$  subtraction. These curves represent the  ${}^2F_{7/2}$  part of the spectrum, which are clearly the sum of two components: an asymmetric fundamental line and a broad satellite.

The asymmetric shape of the fundamental line is not unexpected, since in metals the electron-hole pair excitations across the Fermi level induced by the XPS process are known to lead to such line shapes.<sup>17,18</sup> An analytic expression for such line shapes has been given by Doniach and Sunjic,<sup>19</sup> but it holds only for a model density of states  $\rho(E) = \text{const.}$ , or else should be considered as valid in only a small energy range. A more general procedure has been described by Hopfield<sup>20,21</sup> to obtain the line shape from the density of states. The lower part of Fig. 7 shows the Doniach-Sunjic and the

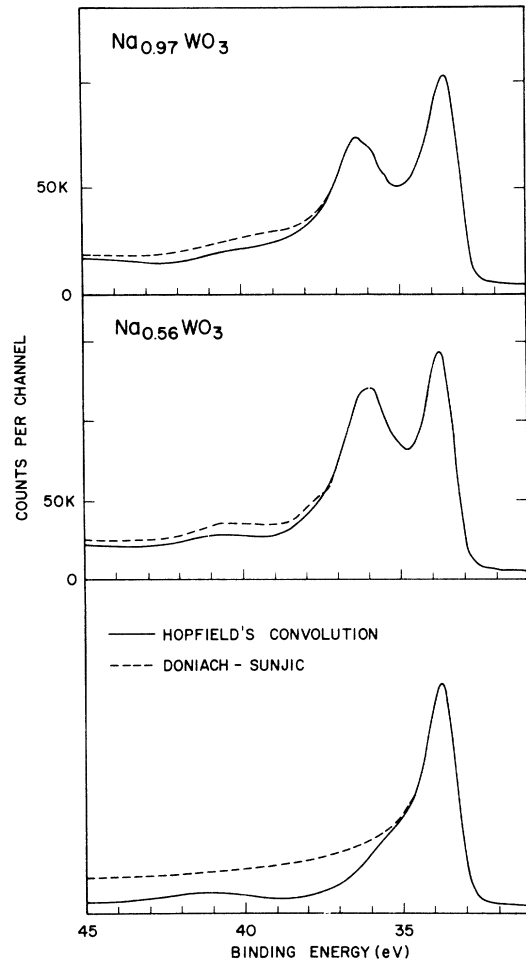


FIG. 7. W 4f spectrum after spin-orbit stripping. These represent the  ${}^7_2$  part of the spectrum. The full line is the final result, the dashed line is obtained by starting from the original data (without W  $5p_{3/2}$  subtraction). The lower part of the figure shows the two possible line shapes used to fit the fundamental line: The dashed line is the Doniach-Sunjic line shape and the full line is obtained from the  $d-d$  density of states using Hopfield's convolution; note the shoulder around 7 eV. Both lines are shown after convolution with the experimental resolution function.

Hopfield line shapes, for  $\alpha=0.4$  both convoluted with the experimental resolution function. There are marked differences between them, the most interesting one being the shoulder at about 7-eV higher binding energy. This feature corresponds to a maximum in the joint density of states, due to the two symmetric sharp peaks in the density of states of the  $\pi$  bands (see Fig. 2). This shoulder is also apparent though weak, in the experimental spectra of Fig. 7. It has also been found in various other core-line spectra of the bronzes, of  $\text{ReO}_3$  and  $\text{WO}_3$  itself. This maximum in the interband

transition probability is observed more directly by optical measurements<sup>14</sup> or electron energy-loss spectroscopy.<sup>15</sup>

## 2. Least-squares analysis

In order to extract quantitative information from the data, a least-squares fit to the W 4*f* spectra was performed. The use of the Hopfield's line shape being hindered by machine time considerations, we contented ourselves with the Doniach-Sunjic line shape in a restricted energy range, though it may yield a systematic (but constant) error in the determination of the parameters of the satellite. This line shape was convoluted with the experimental resolution function. The lifetime and singularity exponent  $\alpha$  were constrained to be the same for the two lines of a given doublet, and the ratio of the  $\frac{5}{2}$  to the  $\frac{7}{2}$  line intensities was constrained to the theoretical value of  $\frac{3}{4}$ . The spin-orbit splitting was allowed to vary, and came out quite reproducibly to be  $2.199 \pm 0.005$  eV. These fits were first performed on the original spectra, and from the approximate parameters obtained, the contribution of the W 5*p*<sub>3/2</sub> lines was calculated and subtracted from the original data, following the procedure described in Appendix B. The final fit was performed on these corrected spectra.

Constant features in these fits throughout the whole  $x$  range are the lifetime broadenings  $\hbar/\tau$  and the singularity exponents  $\alpha$ : the fundamental lines are narrow and strongly asymmetric ( $\hbar/\tau = 0.06 \pm 0.02$  eV,  $\alpha = 0.35$  to 0.40); the satellites are broad and nearly symmetric ( $\hbar/\tau = 0.63 \pm 0.05$  eV,  $\alpha = 0.0$  to 0.10). Another constant feature is the extra Gaussian broadening needed to give a good fit ( $\approx 0.7$ -eV full width at half-maximum in-

stead of the 0.6 eV resolution function). This may be due to inhomogeneous broadening generated by the disorder in the sodium distribution, but could also be due to experimental artifacts such as cleavage imperfections or macroscopic inhomogeneity of  $x$ . In this respect, one should note that inhomogeneities of  $x$  near the surface might yield an asymmetric line shape,<sup>22</sup> so that the extraordinarily large value of  $\alpha$  might be due only partly to many-body effects.

Changing with  $x$  were found to be the positions of the various lines and their relative intensities. The energy separation between the fundamental lines and their respective satellites are plotted in Fig. 5 as a function of  $x$ . This energy separation increases with  $x$ , but is markedly larger than the plasmon energy  $\hbar\omega_1$ , determined from the Na 1*s* spectra. The absolute intensity ratio is difficult to determine accurately, because the Doniach-Sunjic line shape is not an integrable function, and some cutoff has to be taken. This was done by using the line shape obtained with the Hopfield's convolution procedure. The absolute calibration may be in error by as much as 20%, but in view of the constancy of  $\hbar/\tau$  and  $\alpha$  for the various lines through the whole series, the relative uncertainties are much smaller. The resulting intensity ratios are plotted in Fig. 8 as a function of  $x$ .

Also of interest are the absolute positions of the lines which are shown in Fig. 9. The reference energy has been taken at the Fermi level, which is accurately determined (see Sec. IIIA). On the same scale is shown the theoretical variation of the Fermi energy relative to the bottom of the conduction band (which seems to agree with experiment, see Fig. 3). It is clear from Fig. 9 that the sodium and oxygen core levels shift with  $x$  exactly as does the Fermi energy, and therefore are fixed relative to the band structure. The W 4*f* satellites behave in approximately the same way. In contrast, the W 4*f* fundamental lines go to smaller binding energy as  $x$  increases. The various properties of the W 4*f* spectrum are rather puzzling and are discussed below.

## IV. DISCUSSION OF THE W 4*f* STRUCTURE

A classical way to account for the appearance of splittings in XPS is to invoke the presence of several valence states in the initial state of the material, here for the tungsten ion.<sup>23</sup> In view of the strongly covalent character of the bonding<sup>6,7</sup> such an interpretation seems hardly sensible, at least in its crude form. A more plausible interpretation would be in terms of final-state effects, due to the creation of a localized level by the attractive potential of the core hole (Friedel exciton); this ap-

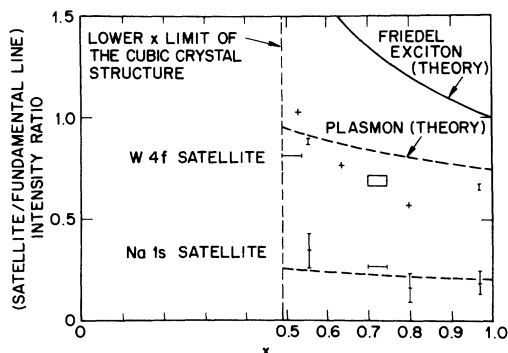


FIG. 8. Intensity ratio  $\beta$  of the satellite to the fundamental line. The dashed lines correspond to the behavior  $\beta \propto x^{-1/3}$  expected from plasmon satellites in a simple metal (vertical scale adjusted for the Na 1*s* satellite only). The full line is an absolute calculation for the W 4*f* satellite in the hypothesis of a Friedel exciton mechanism (see text).

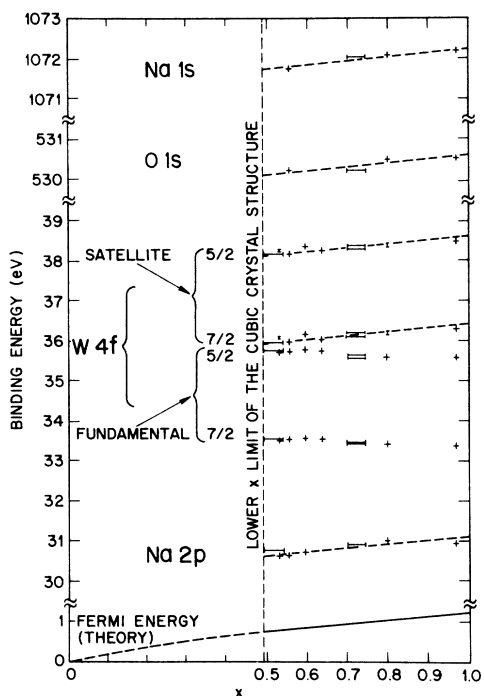


FIG. 9. Positions of the various lines relative to the Fermi level plotted vs  $x$ . The dashed curves have been drawn parallel to the full curve at the bottom of the figure, which represents the Fermi energy as a function of  $x$ . From this figure we conclude that the sodium and oxygen core lines, and also the W  $4f$  satellites, are almost fixed in energy relative to the rigid band structure.

proach provides a more appropriate language for dealing with "valence states" in a covalent material. It is discussed in greater detail below, but satisfactory results are not obtained. As a second approach, we try to link the W  $4f$  satellite with the  $\hbar\omega_1$  plasmon observed on the other XPS lines; the different energy and intensity might be understood as a local effect due to the larger density of conduction electrons on the tungsten sites.

#### A. Friedel exciton mechanism

As first pointed out by Friedel<sup>24</sup> and studied in detail by Combescot and Nozières,<sup>25</sup> the attractive potential of the core hole created upon the XPS process can pull down a localized state from the conduction band. Two lines are observed corresponding to the cases in which the localized state is left full or empty in the XPS transition. Such an interpretation is particularly attractive here, since it might explain the different asymmetries measured for the two lines.<sup>25</sup> The energy splitting between the two lines is the energy difference  $E_F - E_B$  between the Fermi level and the localized

level, and, as will be shown elsewhere,<sup>26</sup> their relative intensities can be related to the filling of the bands in the initial state.<sup>27</sup> Starting from the tight-binding structure of Sec. II and taking the potential of the core hole as a negative site potential  $V$  on a tungsten site, we have determined the energies and wave functions of the localized states by using the Slater-Koster formalism.<sup>28</sup> For each pair of  $\pi$  bands, two localized states were found, one below the filled bonding band, the second in the energy gap between the bonding and antibonding band (see Fig. 10). This state is of special interest here, since its distance to the Fermi energy is in the range of a few eV, and may agree with the observed fundamental-to-satellite splitting.

Numerical calculation indeed showed that taking a site potential  $V = -9.2$  eV on the tungsten site would give good agreement with experiment for the energy splitting (see Fig. 5), and fair agreement for the intensity ratio (see Fig. 8) (not unexpected in view of the experimental uncertainties) *provided the sixfold degeneracy of the ground state is forgotten*. Since the unscreened site potential is estimated to be  $\approx -25$  to  $-30$  eV from the difference in ionization energies between  $W^{4+}$  and  $Re^{5+}$ , a value of  $-9.2$  eV for the screened potential would not be unlikely, and the neglect of the sixfold degeneracy would be justified if it could be proved that the occupancy of one of the six localized states screens out the attractive potential seen by the electrons of the five other subspaces. Although this statement sounds physically right, a self-consistent (unrestricted-Hartree-Fock) calculation of the ground

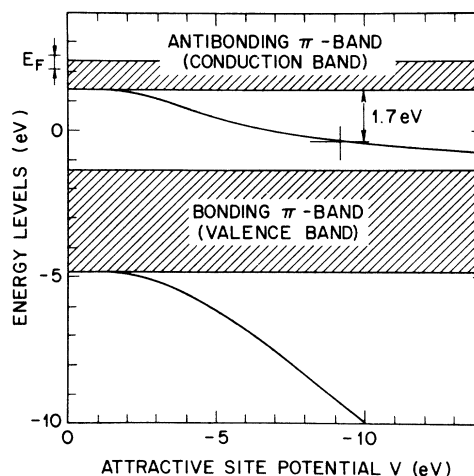


FIG. 10. Localized levels ("Friedel excitons") as a function of the attractive site potential  $V$  on a tungsten site, calculated using the Slater-Koster formalism. The  $\sigma$  bands and the corresponding localized states are not shown, because they are thought to play no essential role.

state failed to give this result.<sup>26</sup> Subsequently, we think that an interpretation of the satellite in terms of a Friedel exciton cannot be entirely correct, and one should look for another explanation.

#### B. W 4f satellite as plasmon excitation

The qualitative similarity of the W 4f satellite with the Na 1s and O 1s  $\hbar\omega_1$  plasmon satellites suggests plasmon excitation as relevant to the W 4f spectrum itself.

The intensity can be understood in terms of the standard theories of intrinsic plasmon excitation in XPS.<sup>29</sup> According to these theories, the ratio  $\beta$  of the first plasmon satellite to the fundamental line increases with decreasing electron concentration, which indeed favors plasmon excitation in the bronzes where the electron concentration is less than one per unit cell. For simple metals, one has  $\beta \sim \frac{1}{6}r_s$ , where  $r_s$  is the average interelectron distance  $(3/4\pi n)^{1/3}$  expressed in atomic units; if this can be applied to the bronzes, it gives  $\beta \approx 0.75x^{-1/3}$  in typical agreement with experiment (see Fig. 8). The smaller value of  $\beta$  for the O 1s and Na 1s lines can be understood as an effect of the band structure on the coupling constant: the wave functions of the conduction band are mainly W-5d-like; hence the density-density correlation function associated with the  $\omega_1$  plasmon excitations is mainly concentrated on the tungsten sites; this makes the coupling constant with plasmons anomalously weak in the case of the oxygen and sodium lines, hence the smaller value for  $\beta$ .

However, at this stage two questions remain unanswered regarding the W 4f spectrum: why is the observed energy shift larger than  $\hbar\omega_1$  (see Fig. 5) and why is only the first "plasmon satellite" observed? (One would expect at least a second satellite of intensity  $\sim \frac{1}{2}\beta^2 \geq 0.3$ , which is clearly absent.)

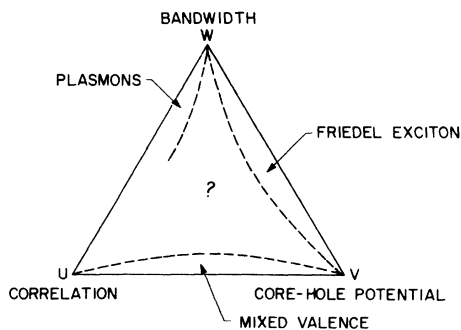


FIG. 11. Nature of the XPS satellites: Schematic diagram of the problem we are faced with. If any one of the three quantities  $U$ ,  $V$ ,  $W$  is negligible, one is near one side of the triangle, which represents a known problem. The case of the bronzes is probably in the central region, where so far no theory is available.

We suggest that the answer to both questions might be in terms of a "localized plasmon."<sup>30</sup> It is known that such excitations are possible and have an energy different from the free plasmon.<sup>30</sup> The occurrence of such an excitation is not unlikely here, since we are in the high-coupling regime  $\beta \geq 1$  and the standard theory of plasmon excitation is known to break down, because of its neglect of certain diagrams.<sup>29</sup> Intuitively, the final state can be visualized as a density oscillation having a strong amplitude on the photoionized tungsten atom; the amplitude clearly cannot exceed the equilibrium electron density  $n$  (negative densities are forbidden!) and this limitation may be associated with the absence of second- and higher-order satellites.

#### C. Discussion

Neither the Friedel-exciton mechanism nor the plasmon interpretation seem to be able to account for the experimental results *quantitatively*, although all the *qualitative* features can be explained by invoking either of these models. The truth is probably that the XPS final state in the tungsten bronzes is a difficult physical problem, because three quantities must be taken into account simultaneously: the potential  $V$  of the core hole, the bandwidth  $W$  (covalency), and the correlation energy  $U$  (which we do not claim to define unambiguously). Figure 11 schematizes the situation: in systems where either  $U$  or  $W$  is negligible, the problem is rather simple, and can be described in terms of either a Friedel exciton, or a mixed valence system (the situation in certain rare-earth materials<sup>31</sup>), respectively. The case  $U \sim W$  without any  $V$  is already a difficult problem of solid-state physics, and here the further complication of  $V$  is added. Although a general solution of the problem is as yet probably beyond our grasp, it should be noted that several perturbational approaches (from the known edges) should be possible, and can constitute interesting theoretical problems.

At the present level, all we can say with confidence is that the W 4f satellite corresponds to an excited state of the screening, and the corresponding excitation is localized and many particle in nature. The "fundamental" and the "satellite" can be referred to as the "screened" and the "unscreened" (or at least "less-screened") final state, respectively.

#### V. CONCLUSION

We have investigated the sodium tungsten bronzes,  $\text{Na}_x\text{WO}_3$ , by XPS in the entire cubic composition range  $0.49 < x < 1.0$ . The band spectrum is

consistent with the theoretical band structure of these materials and gives evidence for the filling of the conduction band with increasing  $x$ . The sodium and oxygen core lines exhibit the distinctive feature of a weak satellite, understood as an excitation of the small-energy plasmon ( $\hbar\omega_1 \sim 2$  eV) characteristic of these compounds. The W 4f spectrum exhibits a structure, which can be analyzed in terms of two doublets. Quantitative agreement with experiment can be obtained neither in the picture of a Friedel exciton nor in terms of a free-plasmon excitation, although either of these explanations predicts the main trends correctly. It is concluded that the right explanation should be a localized many-particle excitation of an intermediate character.

#### ACKNOWLEDGMENTS

The authors are very indebted to Y. Yafet for his constant interest in the theoretical aspects of this work. They also acknowledge valuable discussions with C. Herring, L. Hedin, P. Nozieres, and M. Sunjic.

#### APPENDIX A: DETERMINATION OF $x$

All our samples had been characterized by x-ray lattice-constant measurement. The lattice constant  $a$  is known<sup>32</sup> to give a measure of  $x$  through the relation

$$a = 3.7845 + 0.0820x \text{ \AA}.$$

The XPS observations did not, however, correlate well with these "nominal"  $x$  values. This is not too surprising, because of the inhomogeneity of  $x$  within a given sample, the possibility that XPS probes a sodium-depleted region near the surface, and also the questionability of x-ray data taken on finely crushed powders (the sensitivity of these materials to air exposure might be more important than was thought years ago<sup>9</sup>). Much better correlations were found between the various quantities obtained by XPS, i.e., between the  $\hbar\omega_1$  plasmon energy, the W 4f splitting, and the area of the conduction band spectrum. We therefore decided to rely entirely on the XPS data, which are all taken on the same part of the sample, in the same conditions, and are most likely to be consistent with each other.

The measurement of  $x$  was based on the ratio of the area of the conduction band spectrum to that of the valence band spectrum. These two quantities can be obtained theoretically from the band structure. A plot of their ratio versus  $x$  is shown in Fig. 12. The measurement of this quantity from the experimental spectra was performed in the following way: As a first step the small inelastic

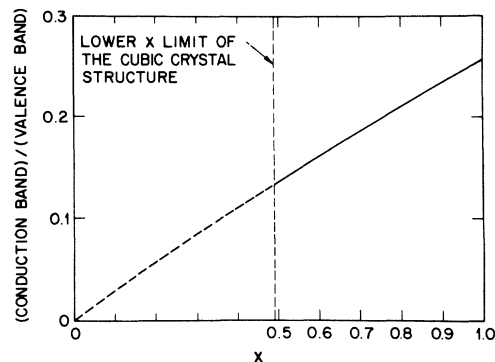


FIG. 12. Theoretical calculation of the ratio of the integrated areas of the XPS spectra of the conduction band and the valence band. This was obtained from the tight-binding band structure of Sec. II and Ref. 7.

background due to the  $\hbar\omega_2$  plasmon excitation was removed from the original data by using a procedure described elsewhere.<sup>33</sup> Then the areas of the conduction-band and valence-band spectra were calculated by assuming a sharp separation located 2.3 eV below the bottom of the conduction band (see Fig. 3). This choice of the limit ensures that the  $\hbar\omega_1$  plasmon satellite of the conduction band spectrum is effectively included in the calculated area of this spectrum, as it should be. The choice of this limit is otherwise somewhat arbitrary and the absolute value of  $x$  obtained by this method might involve some systematic error (as a multiplicative factor). The results were, however, found to be good, both from the point of view of good correlation with other XPS measurements (see the monotonic behavior of other quantities as a function of the so determined  $x$  in Figs. 5, 8, and 9) and even with respect to the absolute magnitude. Our samples are nominally spread over the whole cubic concentration range, and our measured  $x$  values range from 0.49 to 0.97, i.e., just within the limits where this structure is stable, thereby giving a good check of our calibration.

#### APPENDIX B: SUBTRACTION OF THE W $5p_{3/2}$ CONTRIBUTION FROM THE XPS

An ancillary experiment consisted of the observation of the W  $5p_{3/2}$  and W 4f spectra in  $\text{WO}_3$ . In this simpler case, the various lines are well resolved and a fit is unambiguous. The lifetime width of the W  $5p_{3/2}$  line was found to be larger by 1 eV than that of the W 4f lines, and its position was measured to be 4.7 eV above the midpoint of the W 4f doublet.

This information made it possible to subtract the W  $5p_{3/2}$  contribution from the spectra of the bronzes

in the following way: the original data were first fitted up to about 1 eV beyond the maximum of the  $^2F_{5/2}$  satellite (the highest binding-energy line in the  $4f$  spectrum). Using the approximate parameters obtained in that way, the W  $5p_{3/2}$  spectrum was calculated assuming the same (fundamental + satellite) structure as the  $4f$ , taking care of the 1 eV larger lifetime broadening, and the 4.7 eV energy shift, on the basis of the measurements in  $WO_3$ . The intensity was determined by the condi-

tion that the  $5p_{3/2}$  area should be 0.0838 the  $4f$  area, according to the theoretical cross sections,<sup>8</sup> and this for the fundamental and the satellite separately. The small value of this ratio, together with the larger widths of the  $5p_{3/2}$  lines, made the correction rather small (see Figs. 6 and 7) and the final fits, performed after subtraction of this calculated  $5p_{3/2}$  contribution from the original data, usually gave results very similar to the preliminary ones.

\*Present address: Laboratoire de Physique de la Matière Condensée, Ecole Polytechnique, 91120 Palaiseau, France.

<sup>1</sup>See, for example, J. Goodenough, *Progress in Solid State Chemistry*, edited by H. Reiss (Pergamon, Oxford, 1971), Vol. 5, pp. 145-399; and P. Hagemüller, *ibid.*, pp. 71-144.

<sup>2</sup>L. D. Muhlestein and G. C. Danielson, *Phys. Rev.* **158**, 825 (1967).

<sup>3</sup>W. A. Kamitakahara, B. N. Harmon, J. G. Traylor, L. Kopp, and H. R. Shanks, *Phys. Rev. Lett.* **36**, 1393 (1976).

<sup>4</sup>H. R. Shanks (unpublished).

<sup>5</sup>M. Campagna, G. K. Wertheim, H. R. Shanks, F. Zumsteg, and E. Banks, *Phys. Rev. Lett.* **34**, 738 (1975).

<sup>6</sup>L. F. Mattheiss, *Phys. Rev.* **181**, 987 (1969); *Phys. Rev. B* **2**, 3918 (1970); **4**, 3548 (1971).

<sup>7</sup>T. Wolfram, *Phys. Rev. Lett.* **29**, 1383 (1972).

<sup>8</sup>J. H. Scofield, *J. Electron Spectrosc.* **8**, 129 (1976).

<sup>9</sup>G. K. Wertheim, M. Campagna, J.-N. Chazalviel, and H. R. Shanks, *Chem. Phys. Lett.* **44**, 50 (1976).

<sup>10</sup>D. P. Tunstall, *Phys. Rev. B* **11**, 2821 (1975).

<sup>11</sup>J. D. Greiner, H. R. Shanks, and D. C. Wallace, *J. Chem. Phys.* **36**, 772 (1962).

<sup>12</sup>I. Webman, J. Jortner, and M. H. Cohen, *Phys. Rev. B* **13**, 713 (1976).

<sup>13</sup>We are indebted to P. H. Citrin for the *KLL* Auger spectrum of metallic Na which was used to locate the Auger lines in Fig. 4.

<sup>14</sup>D. W. Lynch, R. Rosei, J. H. Weaver, and C. G. Olson, *J. Solid State Chem.* **8**, 242 (1973).

<sup>15</sup>R. E. Dietz *et al.* (unpublished).

<sup>16</sup>This line is readily resolved in the spectra of W or  $WO_3$ .

<sup>17</sup>G. D. Mahan, *Phys. Rev.* **163**, 612 (1967); P. Nozières and C. T. de Dominicis, *ibid.* **178**, 1097 (1969).

<sup>18</sup>G. K. Wertheim and S. Hüfner, *Phys. Rev. Lett.* **35**, 53 (1975).

<sup>19</sup>S. Doniach and M. Sunjic, *J. Phys. C* **3**, 285 (1970).

<sup>20</sup>J. J. Hopfield, *Comments Solid Phys.* **2**, 40 (1969).

<sup>21</sup>See G. K. Wertheim and L. Walker, *J. Phys. F* **6**, 2297 (1976).

<sup>22</sup>If one assumes a depletion of sodium near the surface of the type  $x = x_0 - \Delta x \exp(-z/\delta)$  (where  $x_0$  is the bulk value,  $x_0 - \Delta x$  is the surface value, and  $\delta$  is the thickness of the depletion layer), then given the sampling law of the XPS  $\exp(-z/\lambda)$  (where  $\lambda$  is the electron escape depth), and assuming a linear shift of the XPS line with  $x$ , the line shape turns out to be of the form  $1/(\Delta E)^{1-\delta/\lambda}$ , very similar to a many-body line shape  $1/(\Delta E)^{1-\alpha}$  (the origin of  $\Delta E$  is for  $x_0$ ). This is not conclusive, but suggests that surface effects might be of importance. This is also independently suggested by low-energy-electron-diffraction studies (see Ref. 15) which show a strong  $2 \times 1$  pattern on the (100) face, asserting the different character of the surface.

<sup>23</sup>B. A. De Angelis and M. Schiavello, *Chem. Phys. Lett.* **38**, 155 (1976).

<sup>24</sup>J. Friedel, *Comments Solid State Phys.* **2**, 21 (1969).

<sup>25</sup>M. Combescott and P. Nozières, *J. Phys. (Paris)* **32**, 913 (1971).

<sup>26</sup>J.-N. Chazalviel and Y. Yafet (unpublished).

<sup>27</sup>For example in the case of a narrow unhybridized band (without spin), one finds that the probability of filling the localized state (i.e., the relative intensity of the fundamental line) is proportional to the occupancy of the band: this shows the link between this effect and the concept of "mixed valence."

<sup>28</sup>G. F. Koster and J. C. Slater, *Phys. Rev.* **96**, 1208 (1954).

<sup>29</sup>See, for example, D. C. Langreth, *Nobel Symp.* **24**, 210 (1973).

<sup>30</sup>E. A. Sziklas, *Phys. Rev.* **138**, A1070 (1965).

<sup>31</sup>See, for example, M. Campagna, E. Bucher, G. K. Wertheim, *Struct. Bonding* **30**, 99 (1976).

<sup>32</sup>M. E. Straumanis, *J. Am. Chem. Soc.* **71**, 679 (1949).

<sup>33</sup>J.-N. Chazalviel, M. Campagna, G. K. Wertheim, and P. H. Schmidt, *Phys. Rev. B* **14**, 4586 (1976).